The Journal of Foot & Ankle Surgery 58 (2019) 734–738

Contents lists available at ScienceDirect

The Journal of Foot & Ankle Surgery

journal homepage: www.jfas.org

Computed Tomography Analysis for Quantification of Displacement of the Distal Fibula in Different Foot Positions With Weightbearing and Sequentially Increased Instability: An Anatomic Cadaveric Study on Syndesmosis

Jennifer E. Hagen, MD[1,2], Sascha Rausch, MD[3], Paul Simons, MD[4], R. Geoff Richards, PhD[5], Mark Lenz, MD[6], Matthias Knobe, MD[7], Boyko Gueorguiev, PhD[5], Kajetan Klos, MD[4,8]

[1] *Surgeon, AO Research Institute Davos, Davos, Switzerland*
[2] *Assistant Professor, Department of Orthopedics and Rehabilitation, University of Florida, Gainesville, FL*
[3] *Surgeon, Department of Trauma, Hand and Reconstructive Surgery, University Hospital Jena, Jena, Germany*
[4] *Surgeon, Department of Foot and Ankle Surgery, Catholic Clinic Mainz, Mainz, Germany*
[5] *Professor, AO Research Institute Davos, Davos, Switzerland*
[6] *Surgeon, Private Docent, Department of Trauma, Hand and Reconstructive Surgery, University Hospital Jena, Jena, Germany*
[7] *Surgeon, Professor, Department of Orthopedic Trauma, University of Aachen Medical Center, Aachen, Germany*
[8] *Department of Trauma, Hand and Reconstructive Surgery, University Hospital Jena, Jena, Germany*

ARTICLE INFO

Level of Clinical Evidence: 5

Keywords:
fibular position
imaging under load
ligamentous instability
syndesmotic injuries

ABSTRACT

Syndesmotic injuries are quite common, but accurate diagnosis and treatment can be difficult, in part because of individual anatomic variation and complex movements of the fibula in the incisura. The current cadaveric study was designed to investigate changes in the position of the fibula in the incisura during simulated weightbearing in different foot positions and with sequential sectioning of syndesmotic and deltoid ligaments. Sixteen paired, fresh-frozen cadaveric limbs were embedded in polymethylmethacrylate mid-calf and placed in a weightbearing simulation frame. Computed tomography scans were obtained while the legs were in a simulated foot-flat position (75 N) and single-leg stance (700 N) in 5 foot positions: neutral, 15° external rotation, 15° internal rotation, 20° dorsiflexion, and 20° plantar flexion. The anterior-inferior tibiofibular ligament, posterior tibiofibular ligament complex, deltoid, and interosseous membranes were sectioned sequentially and rescanned. Measurements of fibular diastasis, rotation, anterior-posterior and medial-lateral translation, and fibular shortening were performed. The most destructive state resulted in the largest displacement at the syndesmosis. The degree of subluxation in all ligament states was dependent on the foot position. External rotation created statistically significant displacement at all levels of injury. There were no significant differences between sides of the same donor. Our data demonstrate the importance of foot position in reduction at the syndesmosis under weightbearing. The current ex vivo model could be used to evaluate other aspects of this injury or the value of reconstructive techniques in the future.

The syndesmosis is a complex of strong ligaments that maintain the distal relationship of the tibia and fibula. Injury to the syndesmosis is seen in ~10% to ~13% of all ankle fractures (1) and can also occur independently of bone injury. Although controversy continues with respect to the most appropriate surgical reconstruction of the syndesmosis, most researchers in the field agree with evidence indicating that malreduction and insufficient retention of the syndesmosis lead to poor clinical outcomes and patient pain (2,3). However, there is no consensus to date regarding the anatomical structures of the syndesmosis (4,5). The existence of the inferior transverse ligament as an independent structure or as a part of the posterior tibiofibular ligament (PTFL) continues to be debated. Based on the footprint areas of the ligaments, which are largely proportional to relative strength and stiffness values, the interosseous tibiofibular ligament (ITFL, interosseous membrane) should be the strongest part of the syndesmosis, whereas the PTFL is the second strongest part, and the anterior-inferior tibiofibular ligament (AITFL) is

Financial Disclosure: The authors were not compensated, and no other institutional subsidies, corporate affiliations, or funding sources supported this work, unless clearly documented and disclosed. This investigation was performed with the assistance of the AO Foundation via the AOTRAUMA Network (Grant No.: AR2014_02).

Conflict of Interest: None reported.

Address correspondence to: Sascha Rausch, Department of Trauma, Hand and Reconstructive Surgery, University Hospital Jena, Erlanger Allee 102, 07749 Jena, Germany.

E-mail address: Sascha.Rausch@med.uni-jena.de (S. Rausch).

1067-2516/$ - see front matter © 2018 by the American College of Foot and Ankle Surgeons. All rights reserved.
https://doi.org/10.1053/j.jfas.2018.12.013

the weakest (5). In addition, there is a lack of data regarding the functional behavior of the distal fibula at the level of the syndesmosis. Reported displacements associated with chronic syndesmosis injuries are lateral and posterior translation, as well as shortening and external rotation of the fibula.

The position of the fibula relative to the tibia can be difficult to define in both clinical (6,7) and ex vivo (8) studies. It is believed that external rotation results in the largest and most consistent displacement of the distal fibula. However, the effect of weightbearing remains unclear. In addition, there is considerable variation in the anatomy of the incisura, with the position of the fibula varying from person to person (4,9). Ankle dorsiflexion causes the fibula to rotate externally, which places stress on the AITFL or, in the case of a ruptured AITFL, increases the distance of the ligament footprints. The question of whether isolated injuries to ventral parts of the syndesmosis and its AITFL lead to instability of the joint that would benefit from surgical intervention remains to be elucidated. Functional aspects of the syndesmosis also remain unclear and need to be investigated thoroughly. This cadaveric study was designed to provide detailed information on the changes in the position of the fibula in the syndesmosis during simulated weightbearing in the intact state and with sequential sectioning of the ligaments.

Materials and Methods

Eight pairs of fresh-frozen (−20°C) cadaveric through-the-knee specimens (16 lower limbs in total) were defrosted for 24 hours to 3°C before testing. The donors, 5 males and 3 females, were between 59 and 91 (mean 79.4) years old. The specimens were visually checked for pathology or any prior surgery or trauma, and for integrity of the bones and joints by means of computed tomography (CT). They were embedded mid-tibia in polymethylmethacrylate (SCS-Beracryl D28, Suter Kunststoffe AG, Fraubrunnen, Switzerland), and the fibula was cut at the level of the embedding to be excluded from fixation. The interosseous membrane remained intact.

Each specimen was mounted in a custom-made, air pressure–controlled axial loading frame (Fig. 1). Wooden shanks were used to maneuver the specimens into 5 foot positions (neutral, 15° external rotation, 15° internal rotation, 20° dorsiflexion, and 20° plantar flexion.) Subsequently, CT scans of 0.63-mm slice resolution were obtained for each specimen in a simulated foot-flat condition (unloaded state, 75 N) and single-leg stance (loaded state, 700 N) in all 5 foot positions.

With minimal tissue dissection, the AITFL, PTFL complex, deltoid ligament, and ITFL were sequentially sectioned. The deltoid ligament was sectioned completely around the medial malleolus. The ITFL was sectioned from the tibiofibular articular cartilage all along the incisura fibularis tibiae. Each specimen was rescanned and loaded in all 5 foot positions between each increasing level of destruction. All measurements obtained in the intact unloaded state and loaded ligament-sectioned state were compared to those of the intact loaded state for the respective foot position.

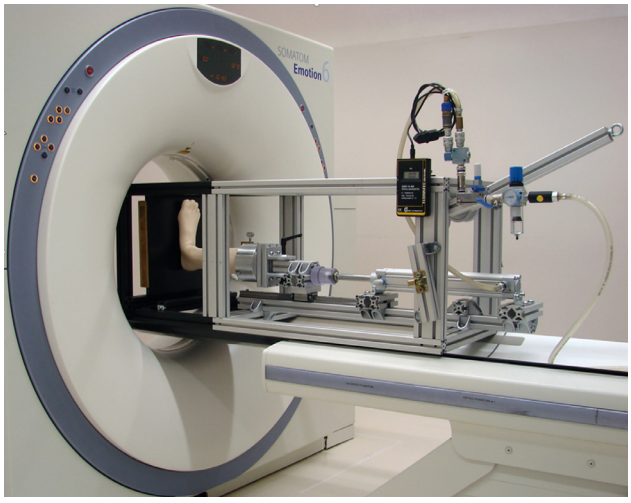

Fig. 1. Custom-made, radiolucent, air pressure-controlled frame with a lower leg model mounted for scanning under axial loading.

Fig. 2. Fibular bimalleolar angle on a coronal computed tomography scan to measure the fibular shortening.

Each CT scan was analyzed using Osirix software (Pixmeo SARL, Bernex, Switzerland). Measurements of fibular diastasis (10), rotation (11), anteroposterior translation, and mediolateral translation (12) were performed on the axial cuts of the CT scans 1 cm proximal to the roof of the plafond. Fibular shortening was measured by approximating the fubular bimalleolar angle on CT (13). The coronal plane was rotated until a mortise view was obtained, and the angle between the distalmost points of the fibula and medial malleolus (fibular bimalleolar angle) was then recorded (Fig. 2).

Statistical analysis was performed using the SSPS software package version 23 (IBM, Armonk, NY, USA). Normality of the data distribution was determined using the Shapiro-Wilk test. The intact and disrupted states regarding each separate parameter of interest were evaluated using the general linear model repeated-measures test, with a Bonferroni post hoc test performed for multiple comparisons. The level of significance was set to $p = .05$ for all statistical tests.

Results

Each series of measurements was reproduced twice. The intra-observer correlation coefficients were 0.99 (diastasis), 0.91 (rotation), 0.98 (anterior-posterior translation), and 0.92 (medial-lateral translation).

The results are presented in Tables 1 and 2. The most destructive state (entire syndesmosis, deltoid, and interosseous membrane resected) resulted in the largest displacement at the syndesmosis, but the extent of subluxation in all ligament states was dependent on the foot position. External rotation created a statistically significant ($p < .05$) malreduction for all positional measurements after all levels of ligamentous injury, except for the fibular bimalleolar angle (Table 1). Dorsiflexion was the second most common foot position creating a positional change in the distal fibula. Plantar flexion significantly affected mediolateral translation and diastasis, even when compared to the intact foot-flat (unloaded) state. Side-to-side comparisons of paired limbs from the same donor revealed no significant differences between the measurements at the same foot position and section state ($p \geq .23$).

To account for anatomic variation between the cadavers, the change in the measurements from the intact loaded state and each resection

Table 1
Statistical comparisons of the fibular measurements. *p* Values for diastasis, rotation, anterior-posterior translation, medial-lateral translation, and fibular bimalleolar angle in the 5 foot positions (neutral, external rotation, internal rotation, dorsiflexion, and plantar flexion) at unloaded (75 N) intact and loaded (700 N) sequentially sectioned states (anterior-inferior tibiofibular ligament → posterior tibiofibular ligament → deltoid → interosseous membrane) versus the loaded intact state in the respective foot position (N = 8 pairs of cadaver limbs)

	Position				
Specimen State	Neutral	ER	IR	DF	PF
Diastasis					
Unloaded intact	.56	.53	.08	.93	<.01†
Loaded sectioned					
AITFL	.49	<.01†	.39	.08	.51
AITFL + PTFL	.81	<.01†	.13	.03*	.02*
AITFL + PTFL + deltoid	.71	<.01†	.03*	<.01†	.02*
AITFL + PTFL + deltoid + IOM	<.01†	<.01†	<.01†	<.01†	<.01†
Rotation					
Unloaded intact	.26	.78	.02*	.02*	<.01†
Loaded sectioned					
AITFL	.08	<.01†	.38	<.01†	.19
AITFL + PTFL	<.01†	<.01†	.58	<.01†	.36
AITFL + PTFL + deltoid	.22	<.01†	.16	<.01†	.52
AITFL + PTFL + deltoid + IOM	.23	.03*	.03*	.02*	.68
AP translation					
Unloaded intact	.65	.44	.03*	.02*	<.01†
Loaded sectioned					
AITFL	.98	<.01†	.75	.07	.71
AITFL + PTFL	.02	<.01†	.21	<.01†	.64
AITFL + PTFL + deltoid	.11	<.01†	.03*	<.01†	.42
AITFL + PTFL + deltoid + IOM	<.01†	<.01†	.04*	<.01†	.34
ML translation					
Unloaded intact	.41	.19	.67	.65	**.04**
Loaded sectioned					
AITFL	.96	**<.01**	.33	**<.01**	.28
AITFL + PTFL	.13	**<.01**	.36	**<.01**	**.02**
AITFL + PTFL + deltoid	.18	**<.01**	.21	**<.01**	**.03**
AITFL + PTFL + deltoid + IOM	**<.01**	**<.01**	**<.01**	**<.01**	**<.01**
Fibular bimalleolar angle					
Unloaded intact	.82	.62	**<.01**	.54	**.04**
Loaded sectioned					
AITFL	.85	.14	**.03**	.14	.29
AITFL + PTFL	.38	.09	.67	.92	.17
AITFL + PTFL + deltoid	.85	.63	.71	.31	.07
AITFL + PTFL + deltoid + IOM	.32	.06	**.04**	**<.01**	**.11**

Abbreviations: AITFL, anterior-inferior tibiofibular ligament; AP, anterior-posterior; DF, dorsiflexion; ER, external rotation; IOM, interosseous membrane; IR, internal rotation; PF, plantar flexion; PTFL, posterior tibiofibular ligament.
Statistically significant at †$p < .01$ and *$p < .05$.

loaded state of every single specimen to its respective intact unloaded state was graphed for each foot position. This allowed us to compare the effects of loading on injury to the more clinically common unloaded CT position. Two representative graphs are shown (Fig. 3). The fibula lateralized most noticeably in the dorsiflexed and externally rotated positions. Rotation of the fibula appeared to follow the position of the foot almost exclusively.

Discussion

We created a clinically relevant weightbearing simulation model for the syndesmosis. The model corroborates common clinical findings and unveils new details about the complex anatomy of this joint. The amount of data on intact positioning and relative motion of the native syndesmosis, although currently limited, is increasing (7,12,14). Previous displacements associated with chronic syndesmosis injuries were lateral and posterior translation, as well as shortening and external rotation of the fibula (15).

Practical observations showed that because of the hexagonal anatomy of the talar dome, forced dorsiflexion of the ankle stressed the mortise and caused fibular displacement (16). Consistent with this finding, we showed increased lateral and posterior translation and external rotation of the fibula with loaded dorsiflexion, in addition to worsening of subluxation in all planes with external rotation. These findings are clinically considered a positive Frick test (17).

Beumer et al (8) assessed the kinematics of the distal tibiofibular joint in cadaveric specimens using radiostereometry and a custom-made testing device that allowed axial loading with 750 N in different foot positions. The authors reported that external rotation resulted in the largest and most consistent displacement of the distal fibula. The effect of weightbearing remained unclear because the load of the ankle did not increase or decrease the displacements of the fibula but rather produced a larger variety of them. In the same study, most testing conditions resulted in cranial displacement or shortening of the fibula. In external rotation and weightbearing, reductions in tibiofibular widths were also observed.

Comparison of our findings with those of Beumer et al (8) revealed inconsistencies for which there are no clear explanations. CT imaging of the syndesmosis should be the standard procedure for obtaining comparable results. Previous research demonstrated that rotational malreduction of the syndesmosis can be reliably measured on axial CT images (18).

According to literature data, the most common type of syndesmotic injury without ankle fracture is a ruptured AITFL resulting from external rotation, such as an “open book” injury (19). Based on the footprint areas of the ligaments, which are largely proportional to relative strength and stiffness values, the ITFL should be the strongest part of the syndesmosis, whereas the PTFL is the second strongest part, and the AITFL is the weakest (5).

Ogilvie-Harris et al (20) measured the lateral traction force required to achieve 2 mm of diastasis after sequential cutting of the various parts of the syndesmosis. The authors reported that the AITFL, ITFL, and PTFL accounted for 35%, 22%, and 42% of total syndesmotic stability, respectively. However, lateral traction does not mirror the functional behavior of the syndesmosis. It is a 3-dimensional problem, and the stability of the syndesmosis results not only from the thickness of its ligaments but also from the tension created by all the ligaments in different foot positions.

Nault et al (7) performed the first in vivo study on the impact of ankle position (sagittal plane) on the distal tibiofibular relationship in a healthy ankle joint. In this radiologic study, 33 volunteers underwent ankle magnetic resonance imaging while placing their feet in different positions. The results revealed an increase in external rotation and lateral translation of the distal fibula during dorsiflexion of the ankle. The authors concluded that syndesmotic imaging studies should take account of the ankle position. Such studies would allow for a better understanding of the functional behavior of the syndesmosis.

One of the most relevant findings from the present study was the impact of an isolated AITFL injury. Controversy surrounds the appropriate treatment for injuries, such as those of the AITFL, that are difficult to diagnose, even on advanced imaging. Clinical data have demonstrated the presence of cartilage damage in a patient with a chronic AITFL injury (21), although it is widely recommended that acute ruptures of the AITFL should be treated with immobilization (8,22). Our data indicated that holding a foot with anterior syndesmosis injury in an externally rotated position resulted in statistically significant subluxation in all planes, except fibular shortening. Dorsiflexion led to displacement, but the neutral position appeared to be “safe.” Based on this observation, treatment aiming at restoring function is not an option until the stability of the syndesmosis is restored, and fixation of the syndesmosis is advised only in a neutral foot position. Our data strongly support this finding.

Another immediately useful clinical finding of this study was confirmation of the similarity in the anatomy of both ankles of a patient. Previous research reported inconsistencies in the anatomy of the incisura from patient to patient (9). Indeed, our raw data showed marked variability in these measurements between specimens, in addition to a significant amount of motion, even in the intact joint. Some researchers

Table 2
Fibular measurements. Mean values ± standard deviations (ranges) for diastasis, rotation, anterior-posterior translation, medial-lateral translation, and fibular bimalleolar angle in the 5 foot positions (neutral, external rotation, internal rotation, dorsiflexion, and plantar flexion) at unloaded (75 N) intact, loaded (700 N) intact, and loaded sequentially sectioned states (anterior-inferior tibiofibular ligament → posterior tibiofibular ligament → deltoid → interosseous membrane) (N = 8 pairs of cadaver limbs)

	Position				
Specimen State	Neutral	ER	IR	DF	PF
Diastasis, °					
Unloaded intact	73.85 ± 11.82 (52.70 to 95.20)	74.89 ± 11.92 58.20 to 94.80)	72.94 ± 12.46 (56.40 to 97.70)	73.26 ± 12.46 (56.60 to 97.00)	75.59 ± 12.24 (56.20 to 96.30)
Loaded intact	73.64 ± 12.01 (57.60 to 95.40)	74.68 ± 12.17 (57.30 to 95.30)	72.40 ± 12.48 (53.40 to 97.30)	73.24 ± 12.20 (55.90 to 95.60)	74.11 ± 12.29 (55.40 to 94.50)
Loaded sectioned					
AITFL	73.94 ± 12.56 (56.80 to 95.90)	72.62 ± 11.30 (55.10 to 92.80)	71.96 ± 12.05 (55.10 to 92.80)	72.39 ± 11.46 (55.40 to 91.10)	74.36 ± 12.02 (56.20 to 94.40)
AITFL + PTFL	73.51 ± 12.46 (56.30 to 95.20)	72.20 ± 11.62 (55.60 to 95.30)	71.06 ± 12.43 (53.30 to 92.90)	71.97 ± 11.58 (55.50 to 91.20)	72.50 ± 11.27 (55.00 to 93.30)
AITFL + PTFL + deltoid	73.46 ± 12.03 (57.00 to 94.90)	69.97 ± 10.67 (53.60 to 93.50)	70.70 ± 12.07 (50.90 to 90.60)	71.61 ± 11.19 (55.40 to 90.70)	71.19 ± 11.39 (54.30 to 93.40)
AITFL + PTFL + deltoid + IOM	70.56 ± 11.13 (52.60 to 91.50)	67.59 ± 9.91 (55.60 to 92.20)	68.04 ± 11.77 (50.00 to 91.10)	69.07 ± 9.88 (53.00 to 85.00)	68.70 ± 11.63 (50.40 to 90.50)
Rotation, °					
Unloaded intact	8.69 ± 5.13 (1.60 to 18.60)	5.59 ± 5.85 (−4.60 to 16.70)	10.36 ± 5.43 (3.14 to 19.90)	8.62 ± 5.24 (1.01 to 17.50)	9.56 ± 4.87 (1.80 to 19.90)
Loaded intact	9.78 ± 5.50 (1.0 to 21.80)	5.49 ± 5.61 (−4.27 to 15.30)	11.66 ± 5.65 (2.53 to 23.30)	7.47 ± 4.74 (1.00 to 17.20)	10.89 ± 5.40 (3.10 to 23.10)
Loaded sectioned					
AITFL	8.49 ± 6.15 (−2.75 to 21.40)	2.49 ± 5.70 (−9,80 to 13.30)	11.95 ± 5.63 (4.30 to 23.20)	5.51 ± 5.98 (−2.50 to 17.50)	11.41 ± 5.75 (3.10 to 23.70)
AITFL + PTFL	6.41 ± 6.01 (−3.10 to 17.30)	−0.79 ± 6.23 (−12.70 to 9.90)	12.15 ± 6.27 (3.54 to 22.80)	4.60 ± 4.94 (−2.60 to 13.20)	10.01 ± 4.93 (2.00 to 19.20)
AITFL + PTFL + deltoid	8.16 ± 6.22 −3.80 to 20.50)	−0.45 ± 6.84 (−13.50 to 11.20)	12.77 ± 6.57 (4.10 to 24.00)	4.29 ± 5.60 (−4.20 to 14.50)	10.33 ± 4.90 (3.10 to 18.70)
AITFL + PTFL + deltoid + IOM	8.16 ± 6.90 (−4.90 to 19.50)	−0.05 ± 7.23 (−13.1 to 9.70)	13.76 ± 6.65 (5.60 to 23.90)	4.66 ± 6.97 (−7.50 to 17.40)	10.43 ± 6.75 (3.40 to 20.80)
AP translation, mm					
Unloaded intact	2.21 ± 1.28 (0.35 to 4.79)	2.83 ± 1.30 (0.82 to 5.39)	2.02 ± 1.49 (−0.42 to 4.79)	2.41 ± 1.30 (−0.41 to 4.80)	1.91 ± 1.30 (0.12 to 4.13)
Loaded intact	2.31 ± 1.30 (0.11 to 4.98)	2.76 ± 1.17 (0.78 to 5.10)	1.66 ± 1.61 (−0.82 to 4.80)	2.73 ± 1.29 (0.49 to 5.31)	1.44 ± 1.33 (−0.33 to 4.11)
Loaded sectioned					
AITFL	2.31 ± 1.34 (0.25 to 5.43)	3.56 ± 1.37 (0.97 to 5.91)	1.63 ± 1.64 (−0.75 to 5.40)	2.98 ± 1.62 (0.66 to 6.25)	1.49 ± 1.38 (−0.39 to 4.58)
AITFL + PTFL	2.99 ± 1.28 (0.55 to 6.17)	4.83 ± 1.29 (2.24 to 7.02)	1.20 ± 2.03 (−1.71 to 6.28)	3.64 ± 1.76 (1.10 to 7.76)	1.29 ± 1.49 (−0.55 to 5.57)
AITFL + PTFL + deltoid	2.83 ± 1.36 (0.91 to 6.81)	5.03 ± 1.37 (2.32 to 7.81)	1.00 ± 2.14 (−1.89 to 6.57)	3.59 ± 1.95 (0.91 to 8.97)	1.09 ± 1.96 (−1.17 to 6.31)
AITFL + PTFL + deltoid + IOM	4.48 ± 1.42 (1.21 to 8.89)	7.30 ± 1.70 (3.85 to 11.41)	2.51 ± 2.32 (−1.43 to 8.38)	5.91 ± 2.09 (1.62 to 10.91)	0.92 ± 2.17 (2.44 to 6.65)
ML translation, mm					
Unloaded intact	−1.69 ± 1.25 (−3.74 to 1.90)	−2.13 ± 1.21 (−4.03 to 0.51)	−1.75 ± 1.17 (−3.91 to 0.61)	−1.70 ± 1.19 (−3.93 to 0.80)	−2.35 ± 1.20 (−4.03 to 0.49)
Loaded intact	−1.94 ± 1.22 (−3.74 to 0.53)	−2.22 ± 1.17 (−4.22 to 0.53)	−1.72 ± 1.20 (−3.65 to 0.68)	−1.67 ± 1.21 (−3.55 to 0.77)	−2.21 ± 1.20 (−3.58 to 0.22)
Loaded sectioned					
AITFL	−1.94 ± 1.20 (−3.66 to 0.65)	−1.61 ± 1.10 (−3.05 to 0.69)	−1.66 ± 1.17 (−3.38 to 0.80)	−1.41 ± 1.08 (−3.07 to 0.90)	−2.27 ± 1.18 (−3.77 to 0.59)
AITFL + PTFL	−1.66 ± 1.25 (−3.73 to 1.46)	−1.31 ± 1.09 (−3.04 to 1.35)	−1.58 ± 0.93 (−2.99 to 0.38)	−1.11 ± 1.03 (−3.25 to 1.62)	−1.89 ± 1.16 (−3.50 to 0.98)
AITFL + PTFL + deltoid	1.70 ± 1.26 (−3.71 to 1.35)	−1.01 ± 1.12 (−2.66 to 1.40)	−1.47 ± 1.19 (−3.51 to 1.52)	−1.05 ± 1.14 (−2.67 to 1.60)	−1.81 ± 1.24 (−3.60 to 1.57)
AITFL + PTFL + deltoid + IOM	−0.84 ± 1.22 (−3.33 to 2.52)	−0.02 ± 1.16 (−2.40 to 2.47)	−0.53 ± 1.18 (−2.83 to 1.70)	−0.16 ± 1.20 (−2.66 to 2.72)	−1.32 ± 1.19 (−3.49 to 2.27)
Fibular bimalleolar angle, °					
Unloaded intact	13.52 ± 3.96 (6.90 to 24.10)	12.56 ± 3.94 (6.30 to 23.80)	13.53 ± 4.06 (8.50 to 25.60)	13.30 ± 4.13 (8.10 to 25.20)	13.49 ± 4.00 (7.40 to 25.20)
Loaded intact	13.48 ± 3.79 (7.60 to 24.20)	12.46 ± 4.03 (6.50 to 24.00)	14.07 ± 4.12 (8.60 to 25.70)	13.03 ± 4.08 (7.90 to 25.60)	14.04 ± 3.98 (7.50 to 25.50)
Loaded sectioned					
AITFL	13.42 ± 4.51 (7.50 to 27.20)	12.94 ± 4.49 (7.50 to 26.70)	13.66 ± 4.20 (8.70 to 26.40)	13.28 ± 3.95 (7.50 to 24.80)	14.26 ± 4.18 (7.60 to 26.40)
AITFL + PTFL	13.70 ± 4.29 (7.20 to 26.10)	12.91 ± 4.20 (7.10 to 25.20)	14.15 ± 4.17 (8.90 to 26.60)	13.07 ± 4.42 (7.70 to 24.70)	13.66 ± 4.22 (6.70 to 25.50)
AITFL + PTFL + deltoid	13.42 ± 4.55 (6.70 to 27.00)	12.60 ± 4.41 (5.90 to 25.30)	14.20 ± 4.33 (9.30 to 28.00)	14.10 ± 4.25 (6.70 to 25.80)	13.41 ± 4.05 (8.00 to 24.70)
AITFL + PTFL + deltoid + IOM	13.78 ± 4.11 (8.00 to 26.50)	13.18 ± 4.24 (7.70 to 25.90)	14.89 ± 4.10 (9.50 to 27.20)	13.77 ± 4.02 (9.00 to 26.90)	13.42 ± 4.23 (8.10 to 24.80)

Abbreviations: AITFL, anterior inferior tibiofibular ligament; AP, anterior posterior; DF, dorsiflexion; ER, external rotation; IOM, interosseous membrane; IR, internal rotation; ML, medial PF, plantar flexion; PTFL, posterior tibiofibular ligament.

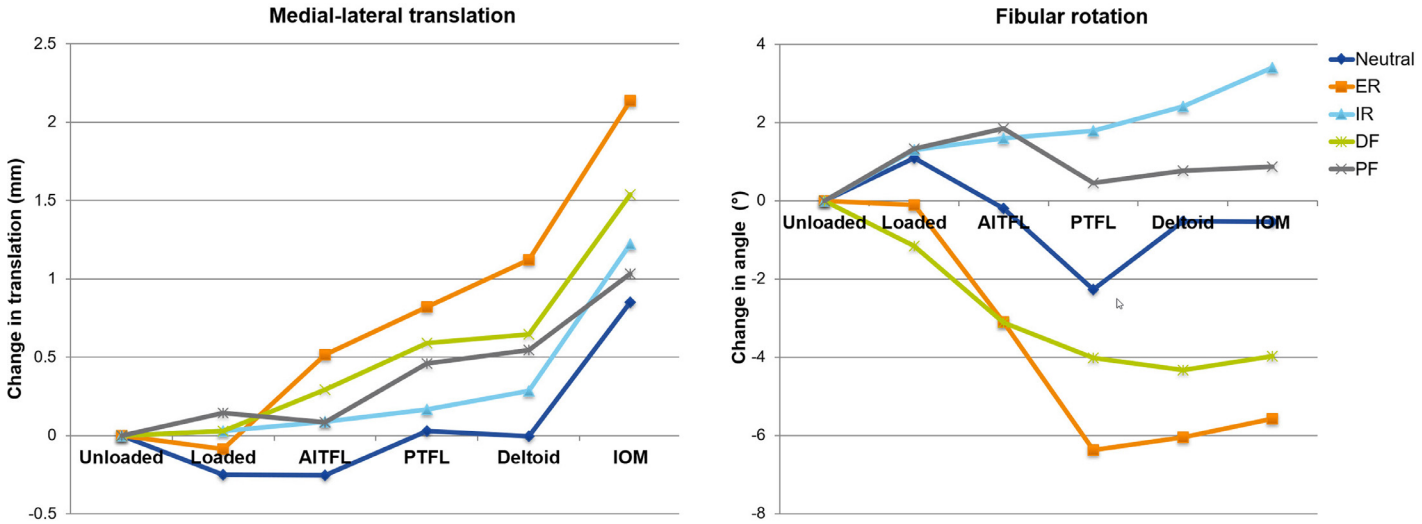

Fig. 3. The mean value of the change in mediolateral translation (left) and fibular rotation (right) in the 5 foot positions (neutral, external rotation [ER], internal rotation [IR], dorsiflexion [DF], and plantar flexion [PF]) at loaded (700 N) intact and sequentially sectioned states (anterior-inferior tibiofibular ligament → posterior tibiofibular ligament → deltoid → interosseous membrane [IOM]) compared to the intact unloaded state (75 N) taken as a baseline. For medial-lateral translation (left), increasing values indicate lateralization; for fibular rotation (right), positive values represent increasing internal rotation, whereas negative values represent external rotation.

have advocated using the contralateral ankle, especially tibia-fibula overlap, on a lateral radiograph to judge where best to place the fibula during fixation (23). Our data confirmed that there were no statistically significant side-to-side differences in the donors, even when comparing extremes of ankle motion, thus, when CT is used for evaluation, it is important to maintain the feet in the same positions or, in cases of preoperative scanning, to keep the uninjured ankle in a neutral position.

The present study has several limitations. Cadaveric studies are incapable of completely simulating the in vivo environment. Although we investigated extremes of foot positioning, it is not the same as gait simulation. These CT scans are merely snapshots of the position of the fibula and do not capture the transitions between positions. Nevertheless, the benefits of this cadaveric model include the ability to collect intact data, as well as the spectrum of injury data. Such data would be difficult, if not impossible, to obtain clinically. A second limitation is that according to preliminary experiments, the tibia was embedded in its middle to rule out any disturbances caused by bending moments caused by the long lever arm of the whole tibia. Therefore, we did not incorporate the stabilizing effects of the proximal tibia-fibula joint into our testing scenario, as our focus was the distal tibio-fibular joint. Although this might change the magnitude of the deformation created at the incisura, we believe that the consistencies between our data and clinical findings justify this model.

In conclusion, we found a clinically relevant simulated weightbearing model for use in studying injuries to the syndesmosis. The data highlight the importance of foot position on the status of the syndesmosis and fibular displacement in the case of isolated AITFL rupture. The data provided by this model are immediately applicable in a clinical setting and may be useful in further investigations. This is a reliable ex vivo model that can be used in the future to evaluate other aspects of syndesmotic injuries or reconstructive techniques.

References

1. Lindsjo U. Operative treatment of ankle fractures. Acta Orthop Scand Suppl 1981;189:1–131.
2. Leeds HC, Ehrlich MG. Instability of the distal tibiofibular syndesmosis after bimalleolar and trimalleolar ankle fractures. J Bone Joint Surg Am 1984;66:490–503.
3. Weening B, Bhandari M. Predictors of functional outcome following transsyndesmotic screw fixation of ankle fractures. J Orthop Trauma 2005;19:102–108.
4. Lilyquist M, Shaw A, Latz K, Bogener J, Wentz B. Cadaveric analysis of the distal tibiofibular syndesmosis. Foot Ankle Int 2016;37:882–890.
5. Williams BT, Ahrberg AB, Goldsmith MT, Campbell KJ, Shirley L, Wijdicks CA, LaPrade RF, Clanton TO. Ankle syndesmosis: a qualitative and quantitative anatomic analysis. Am J Sports Med 2015;43:88–97.
6. Beumer A, Valstar ER, Garling EH, Niesing R, Ranstam J, Löfvenberg R, Swierstra BA. Kinematics of the distal tibiofibular syndesmosis: radiostereometry in 11 normal ankles. Acta Orthop Scand 2003;74:337–343.
7. Nault ML, Marien M, Hébert-Davies J, Laflamme GY, Pelsser V, Rouleau DM, Gosselin-Papadopoulos N, Leduc S. MRI quantification of the impact of ankle position on syndesmosis anatomy. Foot Ankle Int 2017;38:215–219.
8. Beumer A, Valstar ER, Garling EH, Niesing R, Ginai AZ, Ranstam J, Swierstra BA. Effects of ligament sectioning on the kinematics of the distal tibiofibular syndesmosis: a radiostereometric study of 10 cadaveric specimens based on presumed trauma mechanisms with suggestions for treatment. Acta Orthop 2006;77:531–540.
9. Sagi HC, Shah AR, Sanders RW. The functional consequence of syndesmotic joint malreduction at a minimum 2-year follow-up. J Orthop Trauma 2012;26:439–443.
10. Malhotra G, Cameron J, Toolan BC. Diagnosing chronic diastasis of the syndesmosis: a novel measurement using computed tomography. Foot Ankle Int 2014;35:483–488.
11. Phisitkul P, Ebinger T, Goetz J, Vaseenon T, Marsh JL. Forceps reduction of the syndesmosis in rotational ankle fractures: a cadaveric study. J Bone Joint Surg Am 2012;94:2256–2261.
12. Nault ML, Hebert-Davies J, Laflamme GY, Leduc S. CT scan assessment of the syndesmosis: a new reproducible method. J Orthop Trauma 2013;27:638–641.
13. Rolfe B, Nordt W, Sallis JG, Distefano M. Assessing fibular length using bimalleolar angular measurements. Foot Ankle 1989;10:104–109.
14. Mendelsohn ES, Hoshino CM, Harris TG, Zinar DM. CT characterizing the anatomy of uninjured ankle syndesmosis. Orthopedics 2014;37:e157–e160.
15. Kennedy JG, Soffe KE, Dalla Vedova P, Stephens MM, O'Brien T, Walsh MG, McManus F. Evaluation of the syndesmotic screw in low Weber C ankle fractures. J Orthop Trauma 2000;14:359–366.
16. Close JR. Some applications of the functional anatomy of the ankle joint. J Bone Joint Surg Am 1956;38:761–781.
17. Boytim MJ, Fischer DA, Neumann L. Syndesmotic ankle sprains. Am J Sports Med 1991;19:294–298.
18. Knops SP, Kohn MA, Hansen EN, Matityahu A, Marmor M. Rotational malreduction of the syndesmosis: reliability and accuracy of computed tomography measurement methods. Foot Ankle Int 2013;34:1403–1410.
19. Kelikian H, Kelikian AS. *Disorders of the ankle*. Philadelphia, PA: WB Saunders Company; 19851985.
20. Ogilvie-Harris DJ, Reed SC, Hedman TP. Disruption of the ankle syndesmosis: biomechanical study of the ligamentous restraints. Arthroscopy 1994;10:558–560.
21. Wagener ML, Beumer A, Swierstra BA. Chronic instability of the anterior tibiofibular syndesmosis of the ankle. Arthroscopic findings and results of anatomical reconstruction. BMC Musculoskelet Disord 2011;12:212.
22. van den Bekerom MP, Lamme B, Hogervorst M, Bolhuis HW. Which ankle fractures require syndesmotic stabilization? J Foot Ankle Surg 2007;46:456–463.
23. Schreiber JJ, McLawhorn AS, Dy CJ, Goldwyn EM. Intraoperative contralateral view for assessing accurate syndesmosis reduction. Orthopedics 2013;36:360–361.